A microstructure fiber two photon source with conjugate laser pumps

J. Fan[*a], A. Migdall[a], L. J. Wang[b]
[a]Optical Technology Division, National Institute of Standards and Technology
100 Bureau Drive, Mail Stop 8441, Gaithersburg, MD 20899-8441
[b]Max-Planck Research Group for Optics, Information and Photonics, & Univ. of Erlangen,
G.-Scharowsky Str. 1, 91058 Erlangen, Germany

ABSTRACT

We present a systematic experimental study of generating correlated photon pairs using a reversed degenerate four-wave mixing process. By overlapping a pair of parallel- (or cross-) polarized laser pump pulses at conjugate frequencies in a microstructure fiber, parallel- or (cross-) polarized correlated photon pairs are generated at the middle frequency. The generation rate of correlated photons by four-wave mixing with parallel-polarized laser pumps in a 1.8 meter microstructure fiber is comparable or higher than that of a parametric down conversion process in a bulk-crystal at similar pump power levels.

Keywords: four-wave mixing, conjugate frequency, microstructure fiber, photon coincidence.

1. INTRODUCTION

Correlated photons have been used in the study of quantum information science, especially in the areas of quantum communication and cryptography.[1-3] In most experiments, correlated photons are typically generated through parametric down conversion (PDC) of an ultraviolet (UV) beam in a bulk nonlinear crystal. This photon pair generation method was first demonstrated more than three decades ago and has been studied ever since.[4-8] In addition to this method, there are other approaches to generate correlated photons. They include two-photon emission from atoms,[9,10] quantum dots,[11] as well as PDC in engineered crystals such as Periodically Poled Lithium Niobate (PPLN),[12-14] which exhibit higher conversion efficiencies than bulk crystals.

It is of great interest to directly generate correlated photons in fibers. Being part of an optical communication network, correlated photons generated in fibers can be 100% collected and delivered to realize quantum cryptography applications. Compared to conventional fibers, microstructure fiber (MF) has a very large refractive-index contrast between its silica core and its surroundings patterned with air-filled holes, allowing for a very small core size and the associated mode field diameter. This, along with the fact that fiber allows very long interaction lengths, results in high effective optical nonlinearity in a MF at much lower optical pump powers.[15] Also, the MF can be engineered to meet a range of specific applications and pump wavelengths. Overall, this ease of collection, low pump power, and convenient pump wavelength selection make MF an excellent candidate source to provide correlated photons.

It has been demonstrated that by injecting a laser beam (ω_0) into a single mode optical fiber (SMF) or a MF, correlated Stokes (ω_s) and anti-Stokes (ω_{as}) photon pairs at conjugate frequencies are generated via degenerate four-wave mixing process (FWM) at the phase matching condition, $\omega_s+\omega_{as}=2\omega_0$.[16-19] In an ideal single mode fiber (SMF), a mode excited with its polarization along principal axis ***x*** of the fiber does not couple to the mode with orthogonal ***y***-polarization state.[20] This effect has been used to generate polarization-entangled photon pairs by synchronizing two degenerate FWM processes in a dispersion-shifted fiber (DSF).[21,22] In this case, two same-wavelength laser pulses, with polarizations perpendicular to each other, are coupled into a DSF to create correlated photon pairs in the polarization state of $|H_{as}H_s\rangle$ and $|V_{as}V_s\rangle$ which are interferometrically combined, where $|H\rangle$ and $|V\rangle$ are two orthogonally polarized photon states. With proper phase and polarization control, each of the four Bell-states can be prepared. This method is similar to one

* J. Fan's email address is Jfan@nist.gov.

Quantum Communications and Quantum Imaging III, edited by Ronald E. Meyers, Yanhua Shih,
Proc. Of SPIE Vol. 5893, 589309(2005)

where two separate PDC processes are interferometrically combined to prepare a bright polarization-entangled photon pair source using two bulk crystals[7,8] or PPLNs.[14]

In the degenerate FWM process, two photons from the pump field (ω_0) are simultaneously absorbed to create a pair of Stokes and anti-Stokes photons. This process can be reversed. In this paper, we present an experimental study to show that a pair of Stokes and anti-Stokes photons can be annihilated to create two "pump" photons of the same color, $2\omega_0 = \omega_s + \omega_{as}$. These two new photons are necessarily generated simultaneously and hence are correlated, owing to energy conservation.

Normally the generation of correlated photons via FWM in fibers relies on χ_{xxxx} or χ_{yyyy}, a component of the third order nonlinear susceptibility tensor $\chi^{(3)}$, where the photon pairs generated and the pump photons are all co-polarized. In this paper, we also show the generation of cross-polarized correlated photons using χ_{xyxy}, a different component of the susceptibility tensor $\chi^{(3)}$. We overlap a Stokes ($\boldsymbol{E}_s(t,z)$) laser beam polarized along principal axis $\boldsymbol{x}$ with an anti-Stokes ($\boldsymbol{E}_{as}(t,z)$) laser beam polarized along principal axis $\boldsymbol{y}$ in a MF, generating correlated photon pairs by FWM at the middle frequency ω_0 in the state of $|x\rangle |y\rangle$ when phase matching condition is satisfied. Here $|x\rangle$ and $|y\rangle$ are polarization states along axes $\boldsymbol{x}$ and $\boldsymbol{y}$, respectively. The optical field is tightly confined in the small single spatial mode of the MF. The spatial wave function is dropped for simplicity without losing generality. The polarization mode dispersion (PMD) induced temporal distinction between the two photons in polarization states $|x\rangle$ and $|y\rangle$ can be compensated by passing the photons through birefringent optics, such as another piece of MF with appropriate orientation and length. Then at the exit, the two photons are indistinguishable in space, time, and color. This is similar to the generation of correlated photon pairs in a collinear type-II PDC process.[23] Thus, Bell-states can be prepared by postselection 50% of the time, which can then be used to test fundamental quantum mechanics problems such as Bell inequality. This scheme with a pair of orthogonally polarized pump pulses is shown in Fig. 1.

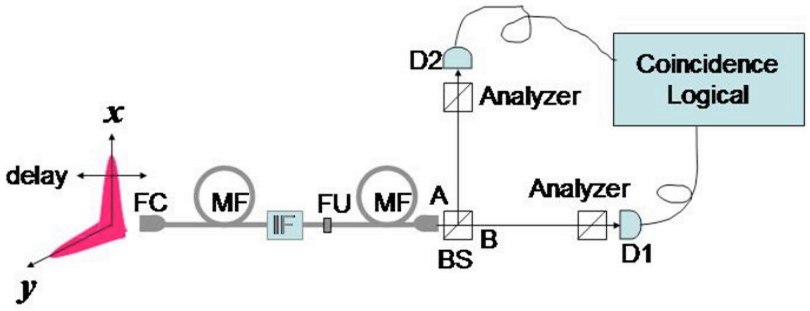

Figure 1: Experimental setup to test Bell inequality. FC: fiber coupler, MF: microstructure fiber (first MF used for generation of cross-polarized photon pairs, second MF for phase compensation), BS: non-polarizing beam splitter, FU: fiber union, IF: interference filter to block the middle frequency, D1 and D2: photon detectors.

2. FWM WITH PARALLEL-POLARIZED LASER PUMPS AT CONJUGATE FREQUENCIES

The experimental setup is shown in Fig. 1. A 3 ps laser pulse with wavelength 835 nm is coupled into microstructure fiber MF1 (835 nm is the zero dispersion wavelength of microstructure fibers: MF1 and MF2[17]) with polarization parallel to one of the principal axes of MF1, driving quasi-continuum generation through FWM and other optical nonlinear mechanisms in MF1. The output from MF1 is collimated and directed onto a high resolution grating (2,200 grooves/mm). Using a two-pass grating configuration and two narrow slits, a pair of pulses at conjugate frequencies: Stokes (837 nm) and anti-Stokes (833 nm) are selected with full-width-at-half-maximum (FWHM) of 0.5 nm. The two-pass arrangement puts these two pulses in the same single spatial mode where they are coupled into a 1.5 m fiber, MF2. Polarizations of these two pulses are parallel to the same principal axis of MF2. We measure the spectra of the FWM output from MF1 and the selected Stokes and anti-Stokes pulses. They are respectively normalized and plotted in the inset of Fig. 1.

The output light pulse from MF2 is again selected using another grating (2,200 lines/mm) and filtered with a narrow slit, only those photons at the wavelength of 834.8 nm are directed to a 50:50 non-polarizing beam splitter (BS). Half of the photon pairs can be split into two single-photon states by the BS, each collected into single mode fiber and detected for photon coincidence measurement with overall detection efficiency of $\eta_1 = 0.042$ or $\eta_2 = 0.063$. In the experiment, the photon count rate at each detector is kept at such a level that, on average, less than 0.05 photon per pulse is emitted at the wavelength of 834.8 nm from the nonlinear optical process in MF2.

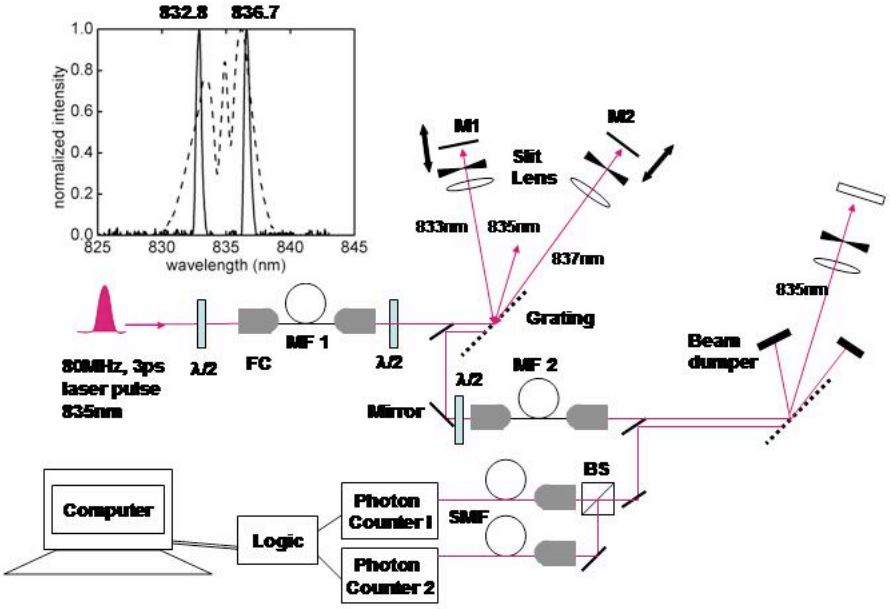

Figure 2: Schematic experimental setup. SMF: single mode fiber, λ/2: half wave plate. M1 and M2 are mirrors. The inset shows the measured normalized spectra. The dashed line indicates the full spectrum of the pulse exiting MF1. The solid line shows the selected Stokes (836.7 nm) and anti-Stokes (832.8 nm) pulse spectra.

As shown in the inset of Fig. 2, the Stokes and anti-Stokes photon wavelengths are only slightly different from the central wavelength (835 nm). The group velocity dispersion is measured and is negligible.[17] The peak pump powers used are low, so that the phase matching condition is automatically satisfied in MF2. The photon pair count rate generated via FWM in MF2 can be estimated as[24]

$$dN/dt \approx \eta\,|\gamma P z|^2\,\Delta\nu\,\tau R, \qquad (1)$$

where $\gamma = \dfrac{2\pi n_2}{\lambda A_{eff}}$ is the nonlinear coefficient. $n_2 \approx 2.8\text{x}10^{-20}$ m^2/W, $A_{\text{eff}} \approx 2.5$ μm^2. The total peak pump power is $P = P_1 + P_2$, with P_1 and P_2 being the peak pump powers of the Stokes and anti-Stokes pulses in MF2. In the experiment, we have $P_1 \approx P_2$. $z = 1.5$ m is the length of MF2. The detection bandwidth $\Delta\nu$ is 86 GHz. The temporal duration of the Stokes and anti-Stokes pulses in MF2 is $\tau \approx 2$ ps. The laser repetition rate is $R = 80$ MHz, and the overall quantum efficiency for detecting a photon pair is $\eta = \eta_1\eta_2/2$.

The coincidence and accidental coincidence rates are plotted as a function of peak pump power P in Fig. 3(a). The accidental rates agree well with the calculated rates $(dN_1/dt)(dN_2/dt)/R$ (dashed line), assuming two independent photon sources. dN_1/dt and dN_2/dt are single photon rates at the two detectors shown in Fig. 3(b). The coincidence rates are smaller than the theoretical values (smooth line) containing both those calculated using Eq.(1) and the calculated accidental rates. This may be due to a number of reasons such as imperfect temporal overlap between the Stokes and anti-Stokes pulses in MF2, which will reduce the final generation rate of correlated photon pairs. The large difference between the measured coincidence and accidental rates shows that a significant number of correlated photon

pairs are generated via FWM in MF2. We further point out that, with the current experimental setup, 440 photon pairs are counted per second at an average pump power of 200 μW (peak pump power 1.25 W) as shown in Fig. 2(a). This is comparable to the count rate of 360,000 per second at average pump power 450 mW in PDC processes in a bulk-crystal,[8] which is equivalent to 160 photon pairs per second at an average pump power of 200 μW.

At low pump power, the gain of the Raman scattering is proportional to P and the gain of FWM is proportional to P^2. We fit dN_1/dt and dN_2/dt with a parabolic function $dN/dt = dN_d/dt + a_1P + a_2P^2$, with dN_d/dt forced to match the count rates due to the dark current and background scattering which is generally negligible. At P = 1.25 W, among all of the generated photons, the fits of dN_1/dt and dN_2/dt consistently give the percentages of the correlated photons as (34 ± 3)% and (32 ± 2)%. This ratio can be also estimated from photon counting,

$$\rho = \frac{1}{R\beta}(C/A - 1)\left(\frac{dN_1/dt}{\eta_1} + \frac{dN_2/dt}{\eta_2}\right), \qquad (2)$$

where C/A is the experimentally measured contrast between the coincidence rate and accidental coincidence rate. Eq. (2) gives a ratio ρ = 16% at P = 1.25 W. This is different from the result obtained using the polynomial fit, and the nature of this discrepancy is not clear.

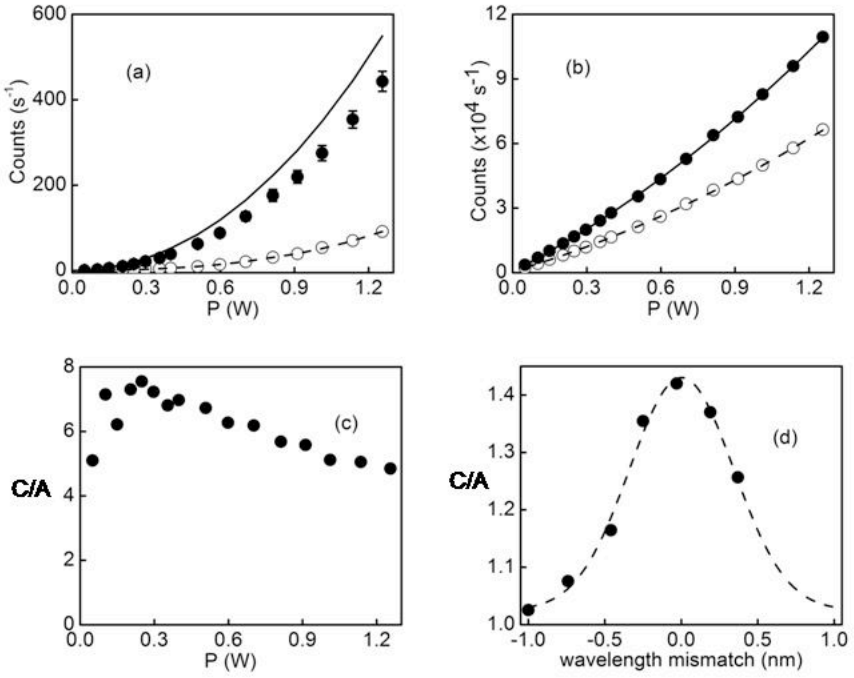

Figure 3: (a) The measured (filled dots) and calculated (smooth line) coincidence rates, and the measured (open dots) and calculated (dashed line) accidental coincidence rates versus P. (b) Single photon count rates (filled and open dots) versus P at two photon counters, fitted with a parabolic function $dN/dt = dN_d/dt + a_1P + a_2P^2$ (solid and dashed lines). (c) Contrast C/A versus P. (d) Contrast C/A (filled bots) versus wavelength mismatch, fitted with a Gaussian function (dashed line). λ_{Stokes}= 836.7 nm with P_1=0.5W; λ_{Stokes} is tuned at around 832.8 nm (corresponding to 0 in wavelength mismatch). P_2 is kept at 0.06 W. Each experimental point in (a)-(d) is taken as a 10-minute average.

Fig. 3(c) shows the contrast C/A as a function of peak pump power with a highest value of approximately 8. The contrast C/A drops with increasing peak pump power. This can be explained by examining the expression of C/A. For low peak power, the contrast C/A can be written as,

$$C/A = 1 + \frac{1}{\Delta\nu\tau}\frac{2\tilde{a}^2}{(\acute{a}_R + 2\tilde{a}^2 Pz)^2}, \qquad (3)$$

where α_R is the gain coefficient of the spontaneous Raman scattering. Eq. (3) shows that the contrast *C/A* monotonically drops with *P*, and (*C/A*-1) is inversely proportional to the product of $\Delta\nu\tau$.

Fig. 3(d) shows a phase-match measurement. This is direct evidence of the FWM process in the second fiber MF2. The narrow spectral width is due to the limited bandwidth shown by the dashed line in the inset of Fig. 2. Furthermore, we have measured the background of stimulated and spontaneous Raman scattering. To do so, we block either one of the signal or idler pulse, and vary the power of the other. In either case, the resulting photon counting rate retains a linear relationship to the peak power showing that stimulated Raman scattering is negligible in the experiment.

3. FWM WITH CROSS-POLARIZED LASER PUMPS AT CONJUGATE FREQUENCIES

For this initial experiment our goal is to examine the generation of cross-polarized photon pairs by FWM with cross-polarized laser pumps in an optical fiber. Different from the experiment arrangement in section 2, here the polarizations of the two selected pulses are parallel to each other and oriented at 45° with respect to axes ***x*** and ***y***. After MF2, we insert a half-wave plate and a polarizing beam splitter (PBS) into the beam path to spatially separate photons of different polarizations (see Fig. 4). We then direct these two beams of different polarizations onto a second grating (2,200 grooves/mm). Using a two-pass grating configuration and two narrow slits, only photons at a wavelength of 834.5 nm are selected and sent to the detectors for coincidence measurements. The collection bandwidth is determined to be 0.2 nm for each of the beam detection channel. Half-waveplates in the beam path are placed to maximize the yield of photons of interest.

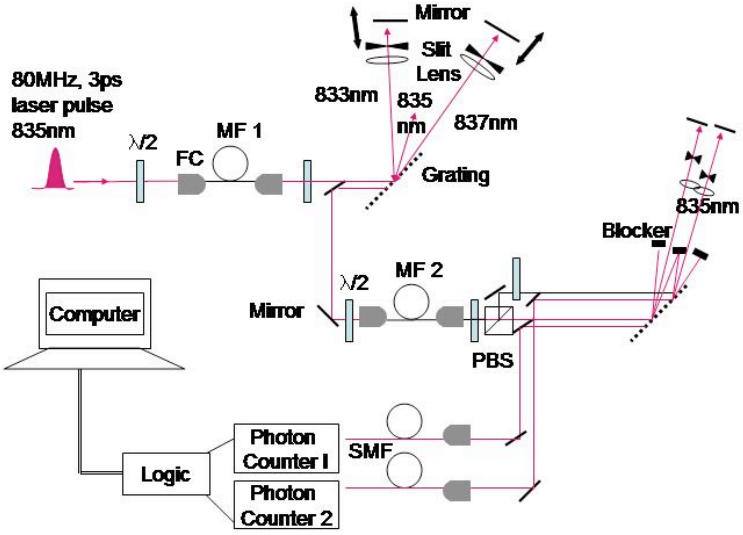

Figure 4: Schematic experimental setup. PBS: polarizing beam splitter.

With polarization oriented at 45° with respect to axes ***x*** and ***y***, the Stokes (anti-Stokes) pulse is split into two pulses of equal power in MF2 polarized along axes ***x*** and ***y***, respectively, resulting in a four-pulse co-propagation configuration in MF2. The electric field of the four-pulse is,

$$\boldsymbol{E}_s(t,z)=E_{sx}(t,z)\boldsymbol{x}+E_{sy}(t,z)\boldsymbol{y}, \quad (4a)$$

$$\boldsymbol{E}_{as}(t,z)=E_{asx}(t,z)\boldsymbol{x}+E_{asy}(t,z)\boldsymbol{y}. \quad (4b)$$

For this short fiber, group velocity dispersion (GVD) is negligible.[17] Pulses polarized along axis ***x*** walk off from pulses polarized along axis ***y*** after propagation in MF2 due to PMD. By adjusting the relative delay of the anti-Stokes pulse with respect to the Stokes pulse in MF2, we can select to overlap either $E_{sx}(t,z)\boldsymbol{x}$ with $E_{asy}(t,z)\boldsymbol{y}$ or $E_{sy}(t,z)\boldsymbol{x}$ with $E_{asx}(t,z)\boldsymbol{y}$. These delay configurations (Fig. 5(a)) are described below.

(1) At delay t_1, only overlap between E_{asx} and E_{sy} occurs. In this case we launch the anti-Stokes pulse ahead of the Stokes pulse into MF2. Cross-polarized photon pairs in the state $|x\rangle|y\rangle$ are generated by FWM at the middle frequency. This is similar to a collinear degenerate type-II PDC process.[23]

(2) At delay t_3, only overlap between E_{asy} and E_{sx} occurs, generating cross-polarized photon pairs in the state $|x\rangle|y\rangle$ at the middle frequency through FWM. In this case, we launch the Stokes pulse ahead of the anti-Stokes pulse into MF2.

(3) At a delay t_2 between t_1 and t_3, we can launch both Stokes and anti-Stokes pulses into MF2 at the same time. Before the PMD walk-off, FWM can occur in both parallel- and cross-polarization schemes. For FWM with parallel-polarized pumps, E_{asx} overlaps with E_{sx} to generate photon pairs in the polarization state $|x\rangle|x\rangle$ along axis $\boldsymbol{x}$, and E_{asy} overlaps with E_{sy} to generate photon pairs in the polarization state $|y\rangle|y\rangle$ along axis $\boldsymbol{y}$. These two processes are coherent to each other and form a superposed state $\frac{1}{\sqrt{2}}(|x\rangle|x\rangle+e^{i\phi}|y\rangle|y\rangle)$ with all photons generated at the middle frequency. This scheme has been used to generate polarization-entangled photon pairs in a DSF.[21,22] Here ϕ is the relative phase due to PMD and the phase difference between the two pumps. FWM also occurs between the cross-polarized pumps. The overlaps of E_{asx} with E_{sy} and E_{asy} with E_{sx} generate correlated photons in the polarization state $|x\rangle|y\rangle$, although the generation rate is one order of magnitude smaller than that of parallel-polarization generation because of $3\chi_{xyxy} \sim \chi_{xxxx}$ (χ_{yyyy}). After PMD walk-off, correlated photon pairs are only generated in the parallel polarization scheme as long as temporal coherence is retained between E_{asx} and E_{sx}, and E_{asy} and E_{sy}.

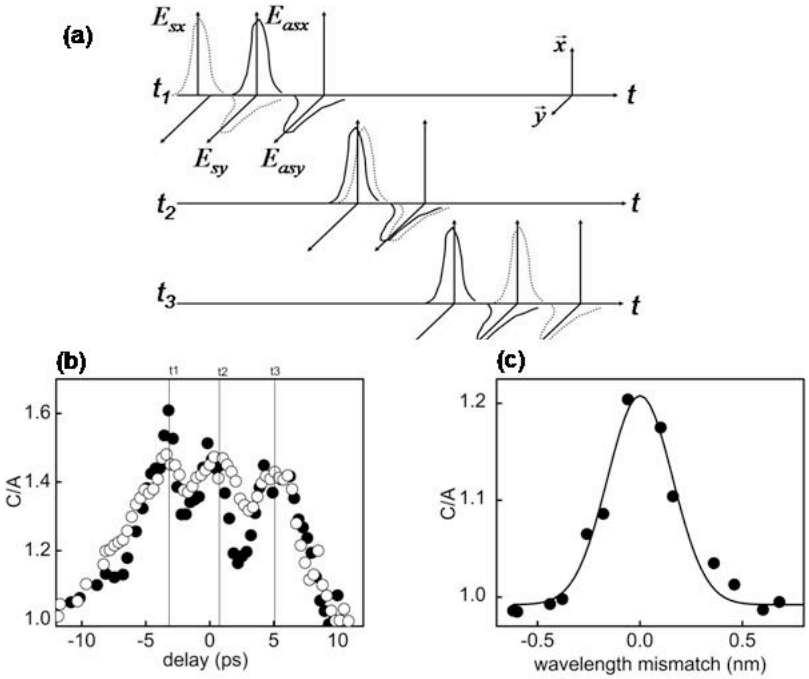

Figure 5: (a) Three cases of two different schemes to generate correlated photons in MF2, with electric field components labeled. Stokes: dashed line, anti-Stokes: solid line. (b) *C/A* versus the relative delay. The filled and open dots are data sets from two separate measurements (2 minute averaging time). The average power for the Stokes and anti-Stokes pulses is ~100 μW for the filled dots and 50 μW for the open dots. (c) Phase-matching measurement (filled dots) at the relative delay time -5 ps, fitted with a Gaussian function (smooth line). The Stokes pump is fixed at the wavelength of 836.3 nm. The anti-Stokes pump is tuned with respect to a central wavelength of 832.7 nm (corresponding to 0 in the wavelength mismatch). Pump condition: Stokes, ~100 μW, anti-Stokes, ~25 μW. The dots are 10 minute measurements.

These three cases are illustrated in Fig. 5(a), in which the PMD walk-offs are exaggerated for better view. In Fig. 5(b), the contrast *C/A* is plotted as a function of the relative delay between anti-Stokes and Stokes pulses. The filled dots and open dots, both exhibiting a three-peak pattern, were obtained from two separate measurements carried out with pump powers different by a ratio of 2. Although the three coincidence peaks are not completely resolved from each other due to limited PMD walk-off in the short fiber, this three-peak pattern results from the three cases discussed above. The coincidence peaks at delay t_1 and t_3 are mainly due to the cross-polarized correlated photons generated by FWM with

cross-polarized pumps. The peak at t_2 is dominated by contribution from $\frac{1}{\sqrt{2}}(|x\rangle|x\rangle+e^{i\phi}|y\rangle|y\rangle)$,[22] generated from FWM with parallel-polarized pumps.

The measured contrast *C/A* in this cross-polarized pump scheme is lower than that (*C/A* ~ 8) of the FWM result with parallel laser pumps discussed in section II. At the same pump power the Raman scattering is same for both polarization schemes, but the FWM gain with cross-polarized pumps is much smaller than the FWM gain with parallel-polarized pumps because of $3\chi_{xyxy} \sim \chi_{xxxx}$. In the experiment, the photon count rate at each detector is nearly linearly proportional to pump power, indicating that Raman scattering dominates. At delay time t_1, with an average pump power of 100 μW, (or a peak power of ~ 0.4 W), the photon count rate is ~ 24 kHz at detector 1 (with an overall detection efficiency of 0.08) and ~ 27 kHz at detector 2 (with an overall detection efficiency of 0.09). The observed photon coincidence rate is ~ 4 Hz (after subtraction of accidental and dark counts).

Because we are more concerned with generation of correlated photons from two cross-polarized laser pumps, we perform a phase-matching measurement at delay t_1, when the *x*-polarized anti-Stokes pulse E_{asx} optimally overlaps the *y*-polarized Stokes pulse E_{sy} in MF2. Fixing the wavelength of Stokes pulse, we saw that the measured contrast *C/A* increases from the baseline (where *C/A* = 1) to the peak and then decreases to the base line again when varying anti-Stokes pulse through the phase-matching wavelength, showing clear evidence of the phase-matching FWM process with cross-polarized pumps in MF2. From the separations of coincidence peaks shown in Fig. 5(b), the mode birefringence of MF2 can be estimated to be $\Delta n \approx 1.6 \times 10^{-3}$.

4. CONCLUSIONS

In conclusion, we have demonstrated a scheme to generate correlated photon pairs using a pair of laser pumps at conjugate frequencies. These correlated photons could be used to prepare Bell-states for a range of applications. It should be noted that the experiments presented here are implemented with limited pump power and relatively short microstructure fibers. Significant efficiency improvements can be made. Because the number of correlated photons generated in fiber is proportional to (γPz),[24] a larger product of γPL will significantly increase the yield of correlated photons. When group velocity dispersion is not a concern, microstructure fiber of longer length will also help to better resolve the two different overlaps. Longer pulse widths with longer overlap times can also help the yield of correlated photons.

ACKNOWLEDGEMENT

This work has been supported by the MURI Center for Photonic Quantum Information Systems (ARO/ARDA program DAAD19-03-1-0199) and the DARPA/Quist program.

REFERENCES

1. C. Kurtsiefer, P. Aarda, M. Halder, H. Weinfurter, P. M. Gorman, P. R. Tapster, "Quantum cryptography: A step towards global key distribution", Nature **419**, 450(2002).
2. M. Aspelmeyer, H. R. Böhm, T. Gyatso, T. Jennewein, R. Kaltenbaek, M. Lindenthal, G. Molina Terriza, A. Poppe, K. Resch, M. Taraba, R. Ursin, P. Walther, and A. Zeilinger, "Long-Distance Free-Space Distribution of Quantum Entanglement", Science **301**, 621(2003).
3. I. Marcikic, H. de Riedmatten,W. Tittel, H. Zbinden, M. Legre, and N. Gisin, "Distribution of Time-Bin Entangled Qubits over 50 km of Optical Fiber", Phys. Rev. Lett. **93**, 180502(2004).
4. D. C. Burnham, D. L. Weinberg, "Observation of Simultaneity in Parametric Production of Optical Photon Pairs", Phys. Rev. Lett. **25**, 84(1970).
5. S. Friberg, C. K. Hong, and L. Mandel, "Measurement of Time Delays in the Parametric Production of Photon Pairs", Phys. Rev. Lett. **54**, 2011(1985).
6. S. Friberg and L. Mandel, "Production of squeezed states by combination of parametric down-conversion and harmonic generation", Opt. Commun. **48**, 439(1984).
7. P. G. Kwiat, E. Waks, A. G. White, I. Appelbaum, and P. H. Eberhard, "Ultrabright source of polarization-entangled photons", Phys. Rev. A**60**, R773(1999).
8. C. Kurtsiefer, M. Oberparleiter, and H. Weinfurter, "High-efficiency entangled photon pair collection in type-II parametric fluorescence", Phys. Rev. A **64**, 023802 (2001).
9. E. Brannen, F. R. Hunt, R. H. Adlington, R. W., Hicholls, "Application of Nuclear coincidence methods to atomic transitions in the wavelength range 2000-6000A", Nature **175**, 810 (1955).
10. A. Kuzmich, W. P. Bowen, A. D. Boozer, A. Boca, C. W. Chou, L.-M. Duan, and H.J. Kimble, "Generation of nonclassical photon pairs for scalable quantum communication with atomic ensembles", Nature **423**, 731(2003).
11. C. Santori, D. Fattal, J. Vu, G. S. Solomon, Y. Yamamoto, "Indistinguishable photons from a single-photon device", Nature **419**, 594(2002).
12. S. Tanzilli, F. D. Riedmatten, W. Tittle, H. Zbinden, P. Baldi, M. D., Micheli, D. B. Ostrowsky, N. Gisin, "Highly efficient photon-pair source using periodically poled lithium niobate waveguide", Elec. Lett. **37**, 26(2001).
13. S. J. Mason, M. A. Albota, F. Konig, and F. N. C. Wong, "Efficient generation of tunable photon pairs at 0.8 and 1.6 μm", Opt. Lett. **27**, 2115(2002).
14. F. Konig, E. J. Mason, F. N. C. Wong, and M. A. Albota, "Efficient spectrally bright source of polarization-entangled photons", Phys. Rev. A **71**, 033805(2005).
15. T. A. Birks, J. C. Knight, and P. St. J. Russell, "Endlessly single-mode photonic crystal fibers", Opt. Lett. **22**, 961(1997).
16. M. Fiorentino, P. L. Voss, J. E. Sharping, and P. Kumar, "All-fiber photon-pair source for quantum communication", IEEE Photonics Tech. Lett. **14**, 983(2002).
17. A. Dogariu, J. Fan, and L.J. Wang, "Correlated photon generation for quantum cryptography", NEC R&D Journal **44**, 294 (2003).
18. Jay E. Sharping, J. Chen, X. Li, and P. Kumar, "Quantum-correlated twin photons from microstructure fiber", Optics Express **12**, 3086 (2004).
19. J. G. Rarity, J. Fulconis, J. Duligall, W. J. Wadsworth and P. St. J. Russell, "Photonic crystal fiber source of correlated photon pairs", Optics Express **13**, 534 (2005).
20. G. P. Agrawal, *Nonlinear Fiber Optics*, 2nd ed. (Academic Press, 1995).
21. H. Takesue and K. Inoue, "Generation of polarization-entangled photon pairs and violation of Bell's inequality using spontaneous four-wave mixing in a fiber loop", Phys. Rev. A **70**, 031802(R) (2004).
22. X. Li, P. Voss, Jay. E. Sharping, P. Kumar, "Optical-fiber source of polarization-entangled photon pairs in the 1550 nm telecom band", e-print quantuh/0402191, 2004.
23. T. E. Kiess, Y. H. Shih, A. V. Sergienko, and C. O. Alley, "Einstein-Podolsky-Rosen-Bohm experiment using pairs of light quanta produced by type-II parametric down-conversion", Phys. Rev. lett. **71**, 3893(1993).
24. L. J. Wang, C. K. Hong, and S. R. Friberg, "Generation of correlated photons via four-wave mixing in optial fibers", J. Opt. B: Quantum and Semiclass. Opt., **3**, 346(2001).

Quantum Communications and Quantum Imaging III, edited by Ronald E. Meyers, Yanhua Shih,
Proc. Of SPIE Vol. 5893, 589309(2005)